Magnetic Resonance Materials in Physics, Biology and Medicine
https://doi.org/10.1007/s10334-019-00760-4

RESEARCH ARTICLE

Evaluation of contrast agent dose and diffusion coefficient measurement on vessel size index estimation

Behrouz Vejdani Afkham[1] · Sadegh Masjoodi[1] · Mohammad Ali Oghabian[1] · Seyed Roholah Ghodsi[2] · Mohammad Reza Nazem Zadeh[3] · Ebrahim Esmati[4] · Mostafa Farzin[5] · Maziar Gilasi[6] · Hasan Hashemi[7,8]

Received: 31 January 2019 / Revised: 19 May 2019 / Accepted: 22 May 2019

Abstract

Objectives The goal of this study is to examine the effect of contrast agent (CA) dose and diffusion coefficient on the estimation of vessel size index (VSI).

Materials and methods Three groups of four participants were enrolled in this study and two different experiments were performed. Different dose of CA, namely 0.1 mmol/kg and 0.05 mmol/kg were assessed in two groups of normal subjects. Diffusion coefficient effect was assessed in the third group with high-grade glioma. Imaging included gradient echo and spin-echo DSC and DTI on a 3-T MR Scanner.

Results VSI estimation using half of standard dose of CA showed higher values compared to the application of standard, with a ratio of 2 for the WM and 1.5 for the GM. VSI estimates for tumor tissues (22 μm) were considerably higher compared to contra-lateral Normal-Appearing WM (NAWM, 4 μm, $P < 0.01$) and Normal-Appearing GM (NAGM, 8 μm, $P < 0.04$).

Discussion Application of standard dose for CA injection and also taking into account the effect of diffusion coefficient can lead to a better correlation of VSI with previous theoretically predicted values and improvement of individual diagnostics in tumor evaluations.

Keywords Contrast agent · Dynamic susceptibility contrast · Vessel size index · Diffusion tensor imaging

✉ Hasan Hashemi
Hashemi_mic@yahoo.com

1 Medical Physics and Biomedical Engineering, School of Medicine, Tehran University of Medical Sciences, Tehran, Iran

2 Development Center of Tehran University of Medical Science, Tehran, Iran

3 Research Center for Science and Technology in Medicine, Tehran University of Medical Sciences, Tehran, Iran

4 Radiation Oncology, Cancer Institute, Tehran University of Medical Science, Tehran, Iran

5 Brain and Spinal Cord Injury Research Center, Neuroscience Institute, Tehran University of Medical Sciences, Tehran, Iran

6 Medical Imaging Center, Imam Khomeini Hospital, Tehran, Iran

7 Advanced Diagnostic and Interventional Radiology Research Center (ADIR), Tehran University of Medical Sciences, Tehran, Iran

8 Department of Radiology, Imam Khomeini Hospital, Institute of Tehran University of Medical Sciences, Keshavarz Blvd, Tehran 1417743855, Iran

Introduction

Vessel size index (VSI) measurement is a technique for achieving vascular information non-invasively. In spite of its valuable capacity, due to its theoretical complication, non-availability of the required MR-sequence and the lack of standardized method in data acquisition and post-processing, VSI has not penetrated into the clinical routines, yet. VSI estimation has been established based on the ratio of ΔR_2^* to ΔR_2; the relaxation rates acquired by gradient echo (GE) spin-echo (SE), respectively, following the administration of intravascular paramagnetic CA. The vascular confined paramagnetic agents affect MR-signals of nearby tissue through the inhomogeneous magnetic field [1].

The variations of SE and GE relaxation rates can be measured using dynamic susceptibility contrast (DSC) MRI. Practical measurements for VSI can be performed either by a dual-contrast sequence (hybrid sequence) or by a dual CA injection in two separate acquisitions [2]. The accuracy of the VSI approximations depends on various parameters such as the strength of main magnetic field (B_0), the echo time,

Published online: 03 July 2019

the dosage of administrated CA, and the diffusion coefficient value [3]. Special care should be taken towards the latter parameters. It has been confirmed that reducing dose of CA would compromise the accuracy of VSI estimates [4], but this matter has not been examined clinically. In prior studies, a constant value has been assumed for the whole brain [5], while the diffusion coefficient hypothetically adopts different values in brain tissues, especially in complications such as tumor that undermine the accuracy of VSI estimations for quantification purposes [6].

The aim of this study is to examine the effect of CA dose and diffusion coefficient on VSI estimates. For this purpose, eight healthy subjects are divided into two groups with different CA dose amounts, followed by DSC-MRI image acquisitions. Furthermore, four patients are enrolled for assessing the effect of diffusion coefficient on VSI estimation in normal subjects and the cases of intracranial neoplasms by studying the intracranial mean diffusivity (MD) maps.

Theory

In practice, measuring the transverse relaxation rates using MR imaging encounters two main dephasing mechanisms: microscopic relaxation due to spin–spin interactions; and mesoscopic relaxation due to local inhomogeneity of magnetic field [7, 8] .In the absence of diffusional movements, spin dephasing due to static field Inhomogeneities is principally reversible using refocusing RF pulses in SE sequence. SE, however, cannot refocus displaced spins due to water diffusion, because of a mismatch between the gradient-evoked phases before and after the displacement.

SE signal drops drastically in the vicinity of microvessels ($R < 10$ μm), where the susceptibility induced field gradient is comparable with diffusion length for a given TE [9]:

$$D_l = \sqrt{D \cdot \mathrm{TE}}. \tag{1}$$

Therefore, phase accumulation across the diffusion length (Eq. 1) is the greatest in vicinity of such microvasculatures which leads to a strong relaxation drop by the vessel size [1, 10–12]. It can be inferred that the inhomogeneous areas nearby larger vessels become dominant with respect to diffusion length scale. On the other hand, by increasing the vessels radius, the phase shift decreases. As a consequence, the SE relaxation descends taking the following form [13]:

$$\Delta R_2 = 0.694 \Delta\omega^{2/3} D^{1/3} \mathrm{CBV} R^{-2/3}, \tag{2}$$

where $\Delta\omega$ is the shift in Larmor frequency induced by the susceptibility differences in intra- and extravascular space, D is the diffusion coefficient, CBV is the cerebral blood volume fraction, and R is the vessel radius.

Gradient echo relaxation rate, on the other hand, does not show any sensitivity to a specific vessel radius range. It increases by increasing the radius, ultimately reaching a plateau level due to the TE limitations in a way that field perturbation can be rescaled in larger vessels ($R > 10$ μm). Consequently, GE relaxation rate can be written as [14]:

$$\Delta R_2^* = \frac{2}{3} \mathrm{CBV}\, \Delta\omega. \tag{3}$$

Therefore, the ratio of ΔR_2^* to ΔR_2 contains proper information about the vessel size.

Behavior of NMR signal in magnetically inhomogeneous tissues that surround vascular networks containing paramagnetic CA can be described by two mechanisms, the static-dephasing regime (SDR) and diffusion-narrowing regime (DNR) [15, 16].

Previously proposed model for VSI assumes that SDR condition takes place in micro-vessel environment tissues. To accomplish this, there is some prerequisites such as strong main magnetic field strength (B_0) and high concentration of CA [17].

In this study, Eq. (4) was applied for VSI estimation. This equation is used when CBV is calculated using DSC-MRI data acquisition [18]:

$$R = 0.867(\mathrm{CBV} \cdot D)^{1/2} \cdot \left(\frac{\Delta R_2^*}{\Delta R_2^{3/2}} \right). \tag{4}$$

The ratio of $\Delta R_2^* / \Delta R_2^{3/2}$ during the first pass of the CA bolus shows different response during arterial (ascending branches in Fig. 1b–d) and venous phases (descending branches in Fig. 1b–d) of vascular network, forming a vascular hysteresis loop (VHL).

It had been demonstrated that the shape and directionality of VHL could differentiate brain healthy tissues (where VHL is counter clockwise, Fig. 1b, c) from tumoral tissues (where VHL is clockwise, Fig. 1d). The main reason for such a result in tumor tissues is their higher arterial blood volume fraction [19].

Materials and methods

Participants

Participants included in this study comprised three groups of four individuals. Two different doses of CA were used for two healthy individuals groups (mean age 37, from 25 to 49), each group received its specific dose. CA dose applied here was 0.1 mmol/kg (standard dose) and 0.05 mmol/kg (half of the standard dose).

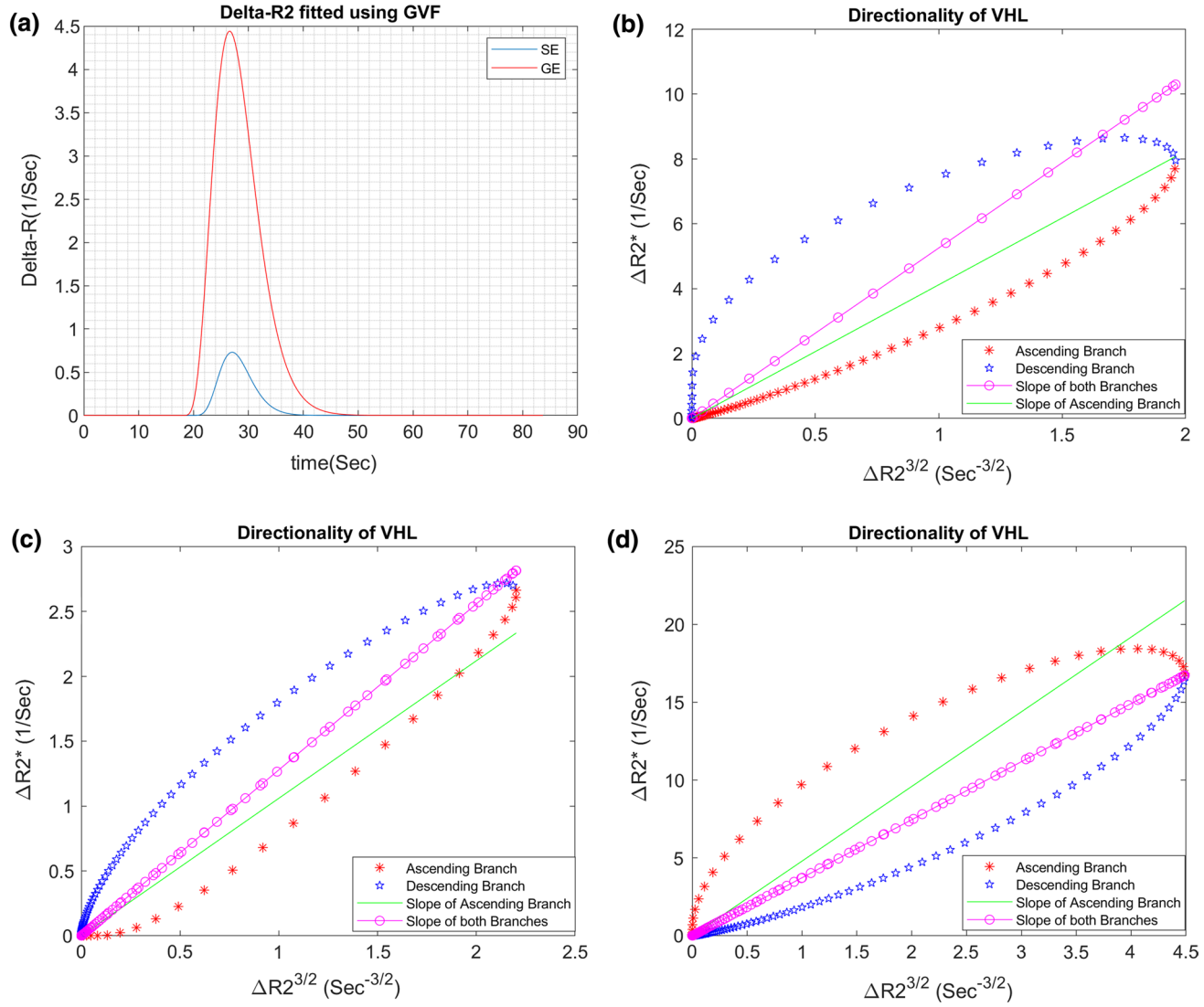

Fig. 1 **a** Delta-R2 relaxation of GE and SE fitted using gamma variate function. **b** Vascular hysteresis loop and linear fitting in normal GM tissue. **c** Vascular hysteresis loop and linear fitting in normal WM tissue. **d** Vascular hysteresis loop and linear fitting in tumor tissue

For second assessment in respect to the effect of the diffusion coefficient on VSI, a third group including patients with high-grade glioma was recruited (mean age 40, from 30 to 51). Standard dose injection was used in all patient groups.

The study was approved by the local committee for medical research ethics (IR.TUMS.MEDICINE.REC.1396.4153). Written Informed consent was obtained from all participants before proceeding with the study.

Imaging protocols

All images were acquired on a 3-T clinical MRI scanner (Discovery MR750, GE Healthcare). One SE DSC and one GE DSC examinations were performed with 60 repetitions and TE for GE/SE: 25/80 ms; TR: 1500 ms; FOV: 240 mm; matrix size: 128×128; and slice thickness: 5 mm. Due to the low sensitivity of spin-echo DSC to the T1-leakage effects, SE images were acquired first [20–22].

Between two DSC acquisitions, DTI was acquired with approximately 10-min length. DTI acquisition was performed with four different *b* values (0, 700, 1500, and 2000 s/mm^2) using 20 non-colinear/planar gradient vectors. Other parameters were as follows: TR: 8000 ms; TE: 128 ms; FOV: 260 mm; matrix size: 256×256; and slice thickness: 3.6 mm.

The slice locations were selected geometrically similar in both DSC-MRI acquisitions. For DTI data acquisition, a whole brain coverage was considered. Structural images include 3D T1-weighted dataset by fast spoiled gradient echo (FSPGR) with TR: 8.4 ms; TE: 3.2 ms; FA: 12°; TI: 450 ms; FOV: 256 mm; and slice thickness: 1 mm. In

addition, FLAIR images were obtained to extract ROIs in tumor areas where a non-enhanced tumor was identified with the following parameters: TR: 7000 ms; TE: 140 ms; FA: 160°; TI: 2200 ms; FOV: 220 mm; matrix size: 320 × 224; and slice thickness: 5 mm.

Special cautions were made to properly fix the head before the imaging to minimize the possible head motions during the scans.

Administration of contrast agent

New generation of CA (Gadobutrol; Gadovist®; Bayer Schering Pharma AG, Berlin, Germany) was used due to its high molarity and decent concentration post-intravenous injection [23].

Injections were performed automatically with a 5 ml/s rate followed by a 20 ml saline flush in the same rate using an MR-compatible injector (Ulrich medical, tennessee™).

To compensate any T1 contamination due to CA leakage in cases of disrupted BBB (group 3), injections included 0.025 mmol/kg as a pre-bolus 5 min before the first DSC-MRI acquisition [24, 25]. Contrast injection was performed with a 15-s delay after starting the DSC-MRI acquisitions. The time interval between two DSC scans is long enough to allow for CA to reach a steady-state concentration prior to the second injection and prevent recirculation effect on the second DSC-MRI.

Data analysis

Data preprocessing and analysis were performed using FSL software (University of Oxford) and MatLab (The Math Works, Inc., Natick, MA, USA). For SE and GE images, motion correction was performed with respect to their first time point separately using MCFLIRT FSL tool. Skull stripping was implemented using bet tool and brain-extracted images were used for further analyses.

MD map was derived from DTI model using Explore DTI (http://www.exploredti.com) using four different b values. For further analysis, the MD map and structural images were co-registered to the mean baseline SE images using the FLIRT tool. Motion-corrected GE time-series were used for CBV estimation using PMA software (ASIST-JAPAN). AIFs were selected manually in the M3 segment at the top of the ventricle and perfusion analysis was performed by de-convolving of the time-series by the AIFs. Maps of CBV were calculated based on the integration of tissue impulse response and normalized to the 3% in average normal brain tissue according to previous investigations [26].

ΔR_2 and ΔR_2* maps were calculated from the motion-corrected time-series of SE and GE images using the following equation:

$$\Delta R_{2\,\mathrm{XE}}(t) = \frac{-1}{\mathrm{TE}} . \ln \frac{S_{\mathrm{XE}}(t)}{S_{\mathrm{XE}}(0)}, \tag{5}$$

where XE stands for SE or GE, TE is the echo time, $S(0)$ is the baseline (pre-bolus) signal, and $S(t)$ is the recorded signal at the time of the corresponding sequence.

Baseline signal was determined as the mean of the signals from the 5th to the 15th dynamic volumes. The first four time points were discarded due to the unsaturated signal.

To ensure about SDR occurrence, both Delta-R_2 time-series fitted to gamma variate function (GVF) to extract only the first bolus passage of CA (Fig. 1a).

VSI calculation

The maximum value of $\Delta R_2^{3/2}$ is defined as the separating point between ascending and descending branches of VHL. According to study of Kiselev et al. [6], since native blood magnetic susceptibility (which is non-zero in venous blood) is one of the reasons for VSI to be overestimated, so to exclude venous portion of VHL, linear fitting was done based on the ascending branch of the VHL (Fig. 1b). The obtained slope of the fitted line was used for VSI calculation.

Regions of interest selection

The co-registered post-contrast T1 images were used for segmentation of WM and GM. For this purpose, the FAST tool was applied. For patients, just normal hemispheres were used for WM and GM segmentation and VSI values in those ROIs were used as a reference for comparison with tumor VSI value (Fig. 2a). For each patient, the tumor masks were drawn manually by an expert neuroradiologist based on contrast-enhanced rim in post-injection T1-weighted images (Fig. 2b) and in the area of high signal intensity on FLAIR images in the cases of non-enhancing tumors. If a tumor was spread out to several slices, the entire volume was considered for as the ROI. In two normal groups, whole brain was used for segmentation purpose. VSI values were extracted using MD map and constant diffusion within three ROIs of WM, GM, and tumor.

Statistical tests

Mann–Whitney U test was done and $P < 0.05$ was considered a statistically significant difference.

Results

CA dose effect on VSI estimation

We compared VSI estimations for normal subjects using two different doses of CA and diffusion coefficient obtained by four different b values in two ROIs (WM and GM). We did not observe any significant differences between CBV in

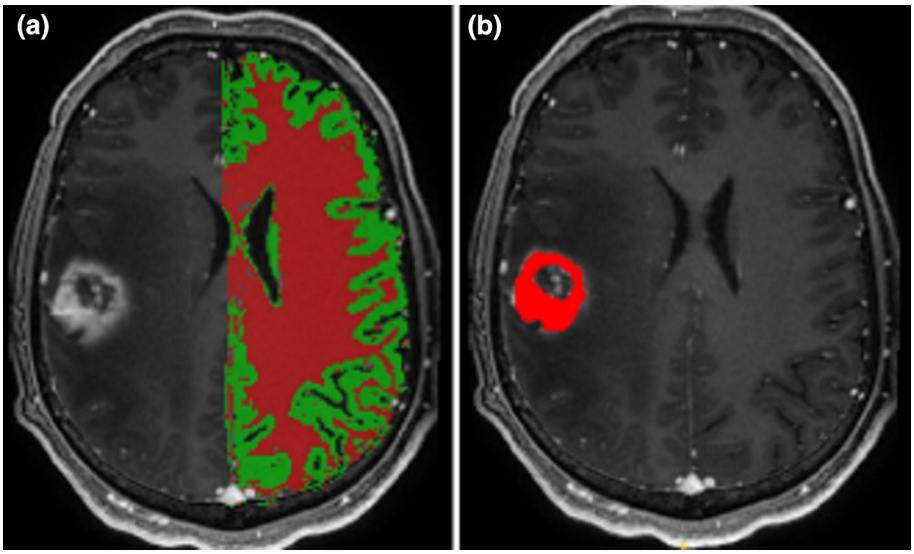

Fig. 2 **a** Graphical presentation of an ROI selection procedure for normal WM and GM. The normal GM and WM were segmented automatically based on the structural MRI in normal contra-lateral hemisphere. The obtained masks were considered as the ROIs. **b** Graphical presentation of an ROI selection procedure for tumor tissues. The ROI was selected manually on the enhanced tumor rim

WM and GM of half dose (1.6 and 2.9%) compared with the standard dose (1.8 and 3%). CBV values were in the same range in normal-appearing tissues in patients group (1.6, 2.7% in NAWM and NAGM, respectively). MD values were also in the same range in WM and GM of standard dose and half-dose groups (0.98 and 1.38 versus 1.04 and 1.47 μm^2/ms in WM and GM, respectively).VSI values in normal-appearing tissues (patients group) were in the same range as were in standard dose group (4 and 8 versus 3 and 9 μm in WM and GM, respectively).

Although CBV values in standard dose and half-dose group were approximately the same, VSI estimation using half of standard dose of CA showed higher values compared to the application of standard, with a ratio of 2 for the WM and 1.5 for the GM (Fig. 3).

The standard deviation of VSI using half-dose injection was greater than that of standard dose (14 and 26 versus 2 and 4 μm in WM and GM, respectively). Apart from low CNR in half-dose acquisition (especially in SE relaxation rate), higher standard deviation could originate from the deviation of static dephasing and lack of linear relationship between CA concentration and relaxation rates in a low dosage of CA.

Diffusion measurement effect on VSI estimation

For evaluation of diffusion coefficient effects on VSI, we calculated MD map by applying four different *b* values. Furthermore, a constant diffusion coefficient (0.8 μm^2/ms) in the whole brain was used in VSI estimation for the comparison purposes.

Although VSI estimation based on constant diffusion is possible, this leads to a less distinction between normal tissues and tumor compared with estimation based on measured mean diffusivity, this differentiation could be worse if VSI estimation was done with half-dose injection.

The constant diffusion coefficient of 0.8 μm^2/ms is more suitable for WM, so we did not observe any differences in VSI of WM when we used this constant value instead of measured mean diffusivity. VSI value in tumoral tissues decreases when constant diffusion assumption is used in Eq. 4 compared with measured MD (14 versus 22 μm), indicating the importance of diffusion influence on the VSI estimations in case of intracranial tumors (Fig. 4).

VSI estimates for tumor tissues (22 μm) were considerably higher compared to contra-lateral normal-appearing WM (NAWM, 4 μm, $P < 0.01$) and normal-appearing GM (NAGM, 8 μm, $P < 0.04$). Furthermore, the vessel radius showed a more heterogeneous pattern in the tumor regions with a wide range from 15 to 50 μm, as a feature of morphological and physiological heterogeneities (Fig. 5) [27]. CBV was considerably higher in tumors ROI ($P < 0.03$) compared to the contra-lateral normal-appearing tissues (5.3 versus 1.6 and 2.7% in NAWM and NAGM, respectively).

Discussion

In this study, we compared VSI estimation in normal subjects and patients with intracranial neoplasms. For both, we evaluated the effect of diffusion coefficient obtained by applying different *b* values. For each of two normal groups, we applied a different dose of CA, while for the tumor patients, a standard CA dose was administrated, assuming a constant diffusion for comparison with VSI values with diffusion coefficient measurement based on DTI model.

The VSI estimation using half of the standard dose of CA (0.05 mmol/kg) showed higher values due to a more decreasing in spin-echo relaxation rate. The calculated values for

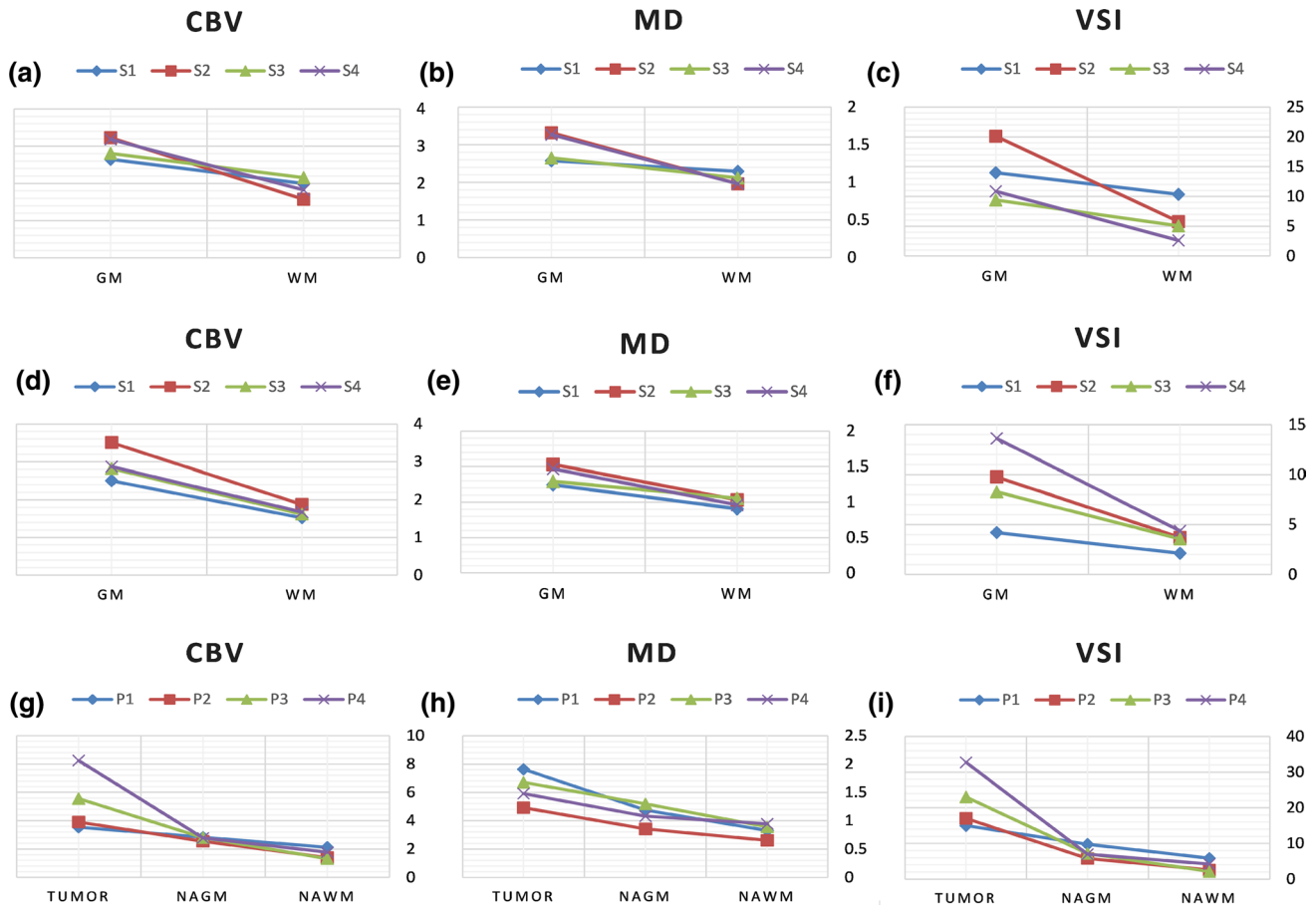

Fig. 3 **a–c** Related to CBV, MD and VSI for half-dose injection. **d–f** Related to CBV, MD and VSI for standard dose implementation. **g–i** Related to CBV, MD and VSI for patients. NAWM and NAGM indicate contra-lateral normal-appearing WM and GM, S1–S4 indicate normal subject's number and P1–P4 indicate patient subject's number. All VSI values are in μm, CBV in % and MD in μm^2/ms

VSI (GM: 9 μm, WM: 3 μm) using MD map and the standard dose of CA in normal subjects is quite close to the theoretical value (7.2 μm) given by Kiselev et al. [6].

Compared with previous MR-VSI studies, our result has a twofold decrement in both normal WM and GM (Table 1). The main reason for this observation is originated from the different methods used for calculation of the ratio of $\Delta R_2^*/\Delta R_2^{3/2}$.

Our proposed method for excluding native blood paramagnetism (fitting the ratio of $\Delta R_2^*/\Delta R_2^{3/2}$ during arterial phase of bolus) results in lower VSI values in normal tissues (where counter-clockwise VHL is expected) and higher VSI values in tumoral tissue (where clockwise VHL is expected) compared to fitting of both branches of VHL. Different loop directions lead to a higher contrast between the normal and tumorous tissue when using the ascending branch.

Since ignoring the native blood paramagnetism (oxygen saturation level) is one of the reasons contributing to VSI overestimation, excluding this effect could be done by fitting the ascending branch of VHL in normal tissues [3, 6].

Our method for CBV estimation (integration of tissue impulse response) was more advanced than Hsu et al. [2] method (integral of ΔR_2^* over the whole curve) [28]. Based on the study of Xu et al. [26], the obtained CBV maps were normalized to 0.03, but the work by Hsu et al. [2] used a normalization factor of 0.06 which leads to higher values of VSI.

In some studies, diffusion coefficient assumed constant 0.8 μm^2/ms, [5, 6], while we emphasized on diffusion measurement for VSI estimation in tumor cases [29].

Diversity of vessel sizes obtained in studies would originate from different data acquisition schemes (i.e., single injection double echo or dual injection, applying pre-bolus injection, assumptions about diffusion coefficient, etc.) and different analysis methods (i.e., VSI estimation based on peak concentration or slope of the line fitted to relaxations time-series, different method for ROI selections, application of deconvolution method for CBV estimation, etc.).

In this study, VSI quantification was performed using a dual injection protocol. The feasibility of such a method for

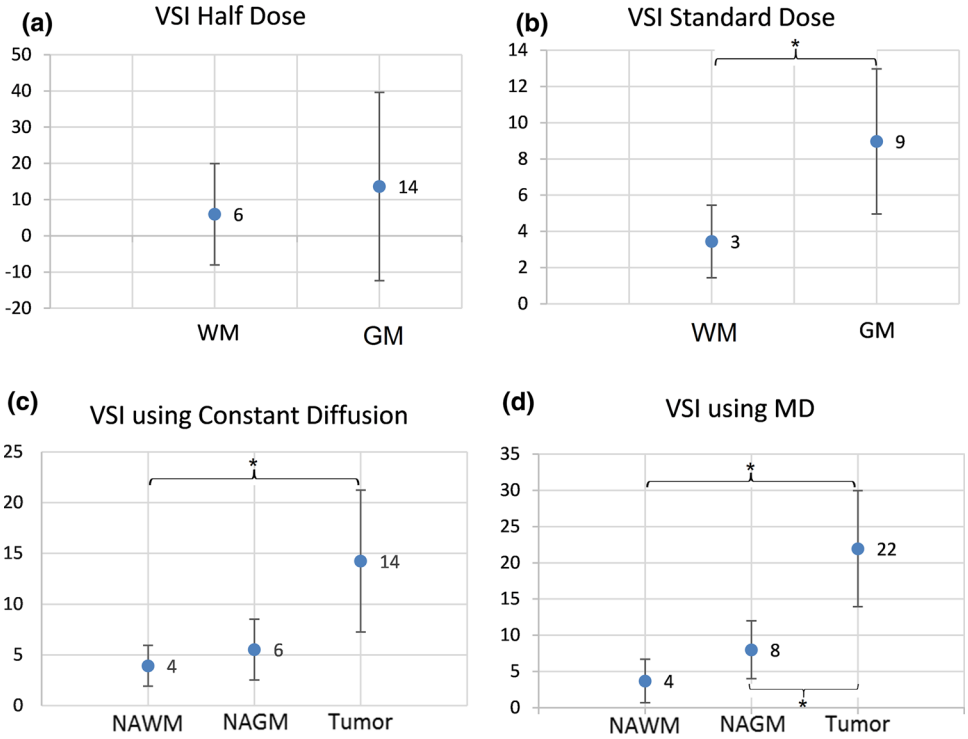

Fig. 4 **a**, **b** Related to mean of estimated VSI in half and standard dose injection. **c**, **d** Related to VSI estimation based on constant diffusion assumption and measured mean diffusivity. The significant level labeled by * is set to be $p < 0.05$. All data are represented as mean ± SD

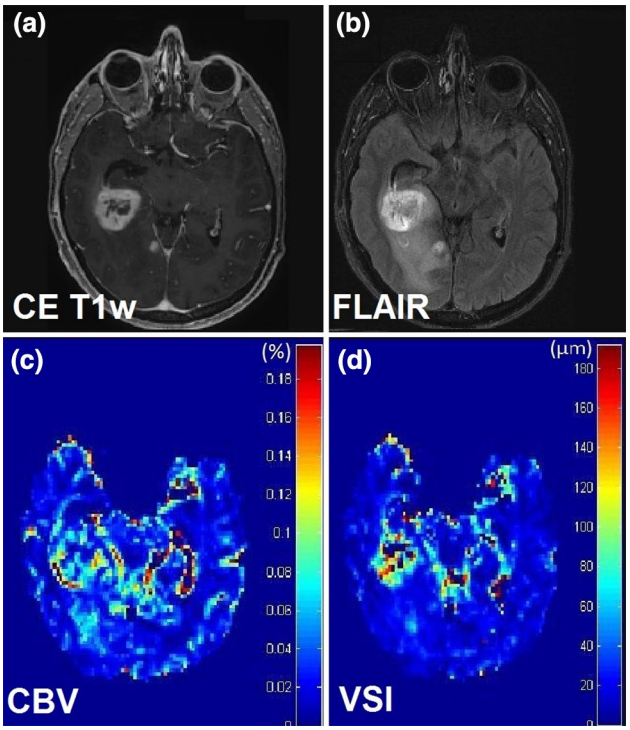

Fig. 5 The images of a patient with anaplastic glioma grade III WHO. **a** Contrast-enhanced T1 weighted. **b** Fat saturated fluid attenuation inversion recovery. **c** Cerebral blood volume. **d** Vessel size index. The color bar encodes the blood volume in % and vessel size in μm

clinically VSI quantification was confirmed in the study of Hsu et al. [2]. There are some challenges such as temporal misregistration between the two DSC time curves and patient motion which can add errors to VSI estimation, if not compensated properly.

By matching the contours in two DSC data, we did not see any significant displacement in two motion-corrected time-series, so we did not apply registration among them (displacement were not more than one voxel in none of our cases).

The effect of temporal misregistration on VSI was also evaluated by Hsu et al. [2], which indicated that time to peak (TTP) differences up to 1 s between two DSC acquisition lead to quantification error within 5%.

However, because we paid careful attention regarding the dynamic EPI acquisitions and also the injection started after tenth time point in both DSC acquisitions, the temporal shift was minimized within 1 s during the first bolus passage. Advantages of the dual injection compared to the single injection dual echo protocol used in prior investigations can be listed as an improvement in SNR, the ability to acquire more slices during the same TR, and the feasibility of applying of the deconvolution (since in double echo schemes TR becomes longer and deconvolution faces with some potential errors) [2, 30].

However, besides the abovementioned reasons for the discrepancy of VSI results across the studies, there are some limitations in acquisition protocols and analytical model following next.

Table 1 VSI in tumor, normal GM and normal WM compared with other studies

ROI	This study (standard dose)		Other studies				
	Slope of ascending branch	Slope of both branch	Kiselev et al. [6]	Hsu et al. [2]	Kellner et al. [30]	Heiland et al. [31]	Kang et al. [5]
Tumor (mean)	22	19	40	105.37	54.76	83.71	109.5
GM (mean)	8	14	18	37.4	–	–	–
WM (mean)	4	6	18.5	15	–	–	–

All the values are in μm

Improvement of the analytical model behind VSI can lead to a better illustration of underlying physiology, especially in tumoral cases where the blood volume fraction may exceed the assumed limit in the modeling. Furthermore, considering vessels orientation with respect to B_0 could be helpful.

In conclusion, this pilot study demonstrates that using constant diffusion coefficient assumption in tumoral tissues for VSI estimation leads to less distinction of the tumor and normal-appearing tissues.

Also, higher values of VSI with higher standard deviation were obtained using half-dose injection. Therefore, data acquisition using standard CA doses and diffusion coefficient measurement for VSI estimation seems to be essential for tumor evaluation. Respecting these covariates, the VSI may serve as an effective tool for the diagnosis of patients with brain neoplasms and for guiding and response assessment after therapeutic approaches as well as biopsy guidance.

Acknowledgements The authors must thank the research affair of Medicine faculty of Tehran University of Medical Sciences, Medical Imaging Center of Imam Khomeini Hospital (Tehran), and all participants in this study.

Author contributions BVA: acquisition of data, analysis and interpretation of data, drafting of manuscript, study conception and design; SM: analysis and interpretation of data, and drafting of manuscript; MAO: study conception and design; SRG: study conception and design; MRNZ: critical revision; EE: critical revision; MF: critical revision; MG: acquisition of data; HH: study conception and design, critical revision.

Funding This research has been supported by Tehran University of Medical Sciences, Grant number 96-03-30-36318.

Compliance with ethical standards

Conflict of interest There is not any conflict of interest to disclose.

Ethical approval The study was approved by the local committee for medical research ethics (IR.TUMS.MEDICINE.REC.1396.4153).

Informed consent Written Informed consent was obtained from all participants before proceeding with the study.

References

1. Boxerman JL, Hamberg LM, Rosen BR, Weisskoff RM (1995) Mr contrast due to intravascular magnetic susceptibility perturbations. Magn Reson Med 34:555–566
2. Hsu Y-Y, Yang W-S, Lim K-E, Liu H-L (2009) Vessel size imaging using dual contrast agent injections. J Magn Reson Imaging 30:1078–1084
3. Tropres I, Grimault S, Vaeth A, Grillon E, Julien C, Payen J-F, Lamalle L, Decorps M (2001) Vessel size imaging. Magn Reson Med 45:397–408
4. Tropres I, Lamalle L, Farion R, Segebarth C, Remy C (2004) Vessel size imaging using low intravascular contrast agent concentrations. Magn Reson Mater Phy 17:313–316
5. Kang H-Y, Xiao H-L, Chen J-H, Tan Y, Chen X, Xie T, Fang J-Q, Wang S, Yang Y, Zhang W-G (2016) Comparison of the effect of vessel size imaging and cerebral blood volume derived from perfusion MR imaging on glioma grading. Am J Neuroradiol 37:51–57
6. Kiselev VG, Strecker R, Ziyeh S, Speck O, Hennig J (2005) Vessel size imaging in humans. Magn Reson Med 53:553–563
7. Kiselev VG (2005) Transverse relaxation effect of MRI contrast agents: a crucial issue for quantitative measurements of cerebral perfusion. J Magn Reson Imaging 22:693–696
8. Willats L, Calamante F (2013) The 39 steps: evading error and deciphering the secrets for accurate dynamic susceptibility contrast MRI: the 39 steps: towards accurate DSC-MRI. NMR Biomed 26:913–931
9. Schmainda KM, Rand SD, Joseph AM, Lund R, Ward BD, Pathak AP, Ulmer JL, Baddrudoja MA, Krouwer HG (2004) Characterization of a first-pass gradient-echo spin-echo method to predict brain tumor grade and angiogenesis. Am J Neuroradiol 25:1524–1532
10. Kennan RP, Zhong J, Gore JC (1994) Intravascular susceptibility contrast mechanisms in tissues. Magn Reson Med 31:9–21
11. Irène T, Pannetier N, Grand S, Lemasson B, Moisan A, Péoch M, Rémy C, Barbier EL (2015) Imaging the microvessel caliber and density: principles and applications of microvascular MRI. Magn Reson Med 73:325–341
12. Kiselev VG, Posse S (1998) Analytical theory of susceptibility induced NMR signal dephasing in a cerebrovascular network. Phys Rev Lett 81:5696–5699
13. Kiselev VG, Posse S (1999) Analytical model of susceptibility-induced MR signal dephasing: effect of diffusion in a microvascular network. Magn Reson Med 41:499–509
14. Yablonskiy DA, Haacke EM (1994) Theory of NMR signal behavior in magnetically inhomogeneous tissues: the static dephasing regime. Magn Reson Med 32:749–763

15. Kiselev VG, Novikov DS (2002) Transverse NMR relaxation as a probe of mesoscopic structure. Phys Rev Lett. https://doi.org/10.1103/physrevlett.89.278101
16. Kjølby BF, Østergaard L, Kiselev VG (2006) Theoretical model of intravascular paramagnetic tracers effect on tissue relaxation. Magn Reson Med 56:187–197
17. Fredrickson J, Serkova NJ, Wyatt SK, Carano RA, Pirzkall A, Rhee I, Rosen LS, Bessudo A, Weekes C, de Crespigny A (2017) Clinical translation of ferumoxytol-based vessel size imaging (VSI): feasibility in a phase I oncology clinical trial population. Magn Reson Med 77:814–825
18. Pannetier N, Lemasson B, Christen T, Tachrount M, Troprès I, Farion R, Segebarth C, Rémy C, Barbier EL (2012) Vessel size index measurements in a rat model of glioma: comparison of the dynamic (Gd) and steady-state (iron-oxide) susceptibility contrast MRI approaches: dynamic vs steady state VSI. NMR Biomed 25:218–226
19. Xu C, Kiselev VG, Möller HE, Fiebach JB (2013) Dynamic hysteresis between gradient echo and spin echo attenuations in dynamic susceptibility contrast imaging: dynamic hysteresis in double echo DSC imaging. Magn Reson Med 69:981–991
20. Essig M, Wenz F, Scholdei R, Brüning R, Berchtenbreiter C, Meurer M, Knopp MV (2002) Dynamic susceptibility contrast-enhanced echo-planar imaging of cerebral gliomas: effect of contrast medium extravasation. Acta Radiol 43:354–359
21. Shiroishi MS, Castellazzi G, Boxerman JL, D'Amore F, Essig M, Nguyen TB, Provenzale JM, Enterline DS, Anzalone N, Dörfler A, Rovira À, Wintermark M, Law M (2015) Principles of T_2*-weighted dynamic susceptibility contrast MRI technique in brain tumor imaging: principles of T_2*-weighted DSC-MRI. J Magn Reson Imaging 41:296–313
22. Carroll TJ, Horowitz S, Shin W, Mouannes J, Sawlani R, Ali S, Raizer J, Futterer S (2008) Quantification of cerebral perfusion using the "bookend technique": an evaluation in CNS tumors. Magn Reson Imaging 26:1352–1359
23. Essig M, Shiroishi MS, Nguyen TB, Saake M, Provenzale JM, Enterline D, Anzalone N, Dörfler A, Rovira À, Wintermark M, Law M (2013) Perfusion MRI: the five most frequently asked technical questions. Am J Roentgenol 200:24–34
24. Leu K, Boxerman JL, Ellingson BM (2017) Effects of MRI protocol parameters, preload injection dose, fractionation strategies, and leakage correction algorithms on the fidelity of dynamic-susceptibility contrast MRI estimates of relative cerebral blood volume in gliomas. Am J Neuroradiol 38:478–484
25. Kim YS, Choi SH, Yoo R-E, Kang KM, Yun TJ, Kim J, Sohn C-H, Park S-H, Won J-K, Kim TM, Park C-K, Kim IH (2018) Leakage correction improves prognosis prediction of dynamic susceptibility contrast perfusion MRI in primary central nervous system lymphoma. Sci Rep. https://doi.org/10.1038/s41598-017-18901-x
26. Xu C, Schmidt WU, Villringer K, Brunecker P, Kiselev V, Gall P, Fiebach JB (2011) Vessel size imaging reveals pathological changes of microvessel density and size in acute ischemia. J Cereb Blood Flow Metab 31:1687–1695
27. Marusyk A, Polyak K (2010) Tumor heterogeneity: causes and consequences. Biochim Biophys Acta (BBA) Rev Cancer 1805:105–117
28. Perkiö J, Aronen HJ, Kangasmäki A, Liu Y, Karonen J, Savolainen S, Østergaard L (2002) Evaluation of four postprocessing methods for determination of cerebral blood volume and mean transit time by dynamic susceptibility contrast imaging: determination of CBV and MTT by DSC-MRI. Magn Reson Med 47:973–981
29. Jensen JH, Lu H, Inglese M (2006) Microvessel density estimation in the human brain by means of dynamic contrast-enhanced echo-planar imaging. Magn Reson Med 56:1145–1150
30. Kellner E, Breyer T, Gall P, Müller K, Trippel M, Staszewski O, Stein F, Saborowski O, Dyakova O, Urbach H, Kiselev VG, Mader I (2015) MR evaluation of vessel size imaging of human gliomas: validation by histopathology: vessel size imaging of human gliomas. J Magn Reson Imaging 42:1117–1125
31. Heiland DH, Demerath T, Kellner E, Kiselev VG, Pfeifer D, Schnell O, Staszewski O, Urbach H, Weyerbrock A, Mader I (2017) Molecular differences between cerebral blood volume and vessel size in glioblastoma multiforme. Oncotarget 8(7)